Oxygen-Rich Enzyme Biosensor Based on Superhydrophobic Electrode

Yongjiu Lei, Ruize Sun, Xiangcheng Zhang, Xinjian Feng, and Lei Jiang*

In the past two decades, via mimicking the top morphologies of natural nonwetting surfaces,[1,2] artificial substrates with a variety of super-wetting properties have been developed[3–10] for many potential applications.[11–14] Very recently, substrates with underwater superaerophilic and superaerophobic properties were created.[13–15] Superaerophobic substrate has low adhesive force to gas bubbles, and has shown great potential for the development of electrode where gas-born reaction takes place.[13,14] In contrast, when a substrate with underwater superaerophilicity is immersed in aqueous solution, air pockets will be trapped and a solid–liquid–air three-phase interface will form.[14,15] This offers us an opportunity to address the gas-deficit problem of many reaction systems.

The development of accurate bioassays, particularly enzyme-based ones, is important for the diagnosis of worldwide diabetes and other medical problems.[16–25] In comparison to artificial electron mediators, oxygen is a natural and more effective electron mediator for oxidase. Analyte levels are commonly assayed via the measuring of oxygen consumption or H_2O_2 formation in oxidase-catalyzed bioreactions.[16–18] However, conventional biosensors are based on electrode that has solid/liquid two-phase interface, where oxygen is supplied through liquid phase with low diffusion coefficient, and low and fluctuant concentration. Hence, oxygen required at the enzymatic reaction zone is limited according to Fick's law of diffusion, which makes the detection upper limit of linearity, sensitivity and accuracy restricted. Up to today, it is still a challenge to solve the oxygen-deficit problem.

Here we describe a simple solution by developing an oxygen-rich enzyme biosensor based on superhydrophobic electrode that has solid–liquid–air three-phase interface, where oxygen is sufficient and constant. The schematic representation of the superhydrophobic three-phase (STP) biosensor is illustrated in **Figure 1**. Oxidase is immobilized on a superhydrophobic substrate that modified with H_2O_2 catalyst. The superhydrophobic substrate can be fabricated based on the cooperative effect between micro-/nanocomposite surface structure and low surface energy materials.[1,2] When such biosensor is immersed in analyte solution, air pockets will be trapped underneath because of the substrate's underwater superhydrophobicity.[14,15] Figure 1b is an enlarged view of the solid–liquid–air three-phase assaying interface, where oxygen can diffuse directly from air phase to the oxidase active sites. Because of the much higher diffusion coefficient of oxygen in air (2.0×10^{-1} cm^2 s^{-1}) than that in liquid (≈2.1×10^{-5} cm^2 s^{-1}),[26] oxygen level at the three-phase reaction zone can be several orders of magnitude higher. This allows free diffusion of analyte and ensures large amount of H_2O_2 formation for accurate analyte levels determination.

Based on the model reasoned above, many types of STP-biosensors can be fabricated, given the availability of a wide variety of oxidases, assaying approaches, H_2O_2 catalysts and superhydrophobic substrates. In this study, to demonstrate the biosensor model, we fabricated electrochemical STP-biosensor by immobilizing glucose oxidase (GO*x*) on Pt catalysts modified conducting superhydrophobic carbon fiber mesh. The GOx catalyzed reaction product of H_2O_2 is electroxidized on Pt surface to give fast current response for glucose level determination. As shown in **Figure 2**a, carbon fiber with a diameter of ≈10 μm forms net-structures. Pt catalysts with sizes ranging from 50 to 300 nm were electrodeposited on the surface of the topmost layer of fibers (Figure 2b,c). Each of these Pt particles is composed of nanoflakes with thickness of about 9 nm. Such micro/nanoscale structure prevents water from wetting as shown in Figure 2e (a nearly spherical water droplet suspended on the electrode substrate). Figure 2f and Figure S1 (Supporting Information) are environmental (E) SEM images of GO*x*/chitosan composite film coated electrode substrate. The composite film is very thin (~200 nm) and well-separated from the substrate by hierarchical Pt particles. Such electrode architecture facilitates free diffusion of oxygen and glucose from air and liquid phases to the assay interface, respectively.

The STP-biosensor was then used to detect glucose. Cyclic voltammograms (CVs) (**Figure 3**a) show that the electroxidation current increase steadily as expected with the increase of glucose concentration up to the value 176 mM. From the calibration plot of current versus concentration shown in Figure 3b, it can be seen that a linear detection range up to 156 mM with a correlation coefficient of 0.999 is achieved. As illustrated in the inset in Figure 3b (dark line), control experiment based on normal electrode (glassy carbon electrode) gives linear detection range up to only about 5 mM. In order to extend the dynamic range of normal biosensors that rely on the use of limited soluable oxygen, thick mass-transport-limiting membranes

Dr. Y. Lei, Prof. X. J. Feng
College of Chemistry
Chemical Engineering and Materials Science
Soochow University
Suzhou 215123, P. R. China
E-mail: xjfeng@suda.edu.cn
Dr. R. Sun, Prof. L. Jiang
School of Chemistry and Environment
Beihang University
Beijing 100191, P. R. China
Prof. X. Zhang, Prof. X. J. Feng
Suzhou Institute of Nano-Tech and Nano-Bionics
Chinese Academy of Sciences
Suzhou 215123, P. R. China

DOI: 10.1002/adma.201503520

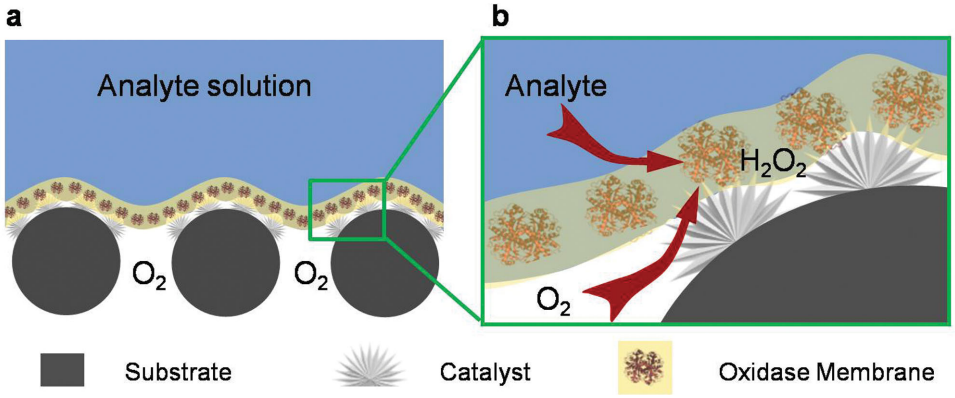

Figure 1. Schematic representation of the STP-biosensor. a) A thin layer of oxidase/chitosan composite film is immobilized on the superhydrophobic substrate that modified with H_2O_2 catalyst. When the electrode is immersed in analyte solution, air phase will be trapped underneath the solution. b) Enlarged view of the solid–liquid–air three-phase reaction zone where oxidase catalytic bioreaction takes place. Oxygen required at the oxidase active sites can diffuse directly from air phase with orders of magnitude higher diffusion coefficient than that from liquid phase. This makes oxidase kinetics no longer oxygen level limited, allows free influx of analyte, and ensures large amount of H_2O_2 production for analyte level measurement.

are commonly used to reduce the influx of glucose and increase oxygen/glucose ratio at the liquid–solid assay interface. Consequently, this results in a very small amount of H_2O_2 production and low sensitivity (~nA/mM). In marked contrast, since oxygen at the reaction zone of STP-biosensor is sufficient, mass-transport-limiting membranes are no longer required here. As shown in Figure 2f, the oxidase/chitosan composite film is only about 200 nm thin, which allows the free diffusion of glucose and the large amount of H_2O_2 production. As a result, much higher detection sensitivity (36 μA mM^{-1}) was achieved in current research. The high sensitivity in turn offers the STP-biosensor a good detection limit. As shown in Figure S2 of the Supporting Information, reproducible amperometric response was recorded with increase of glucose from as low as 50 nM to 0.5 mM, indicating that the linear detection range of STP-biosensor can be from as low as nano-mol up to 156 mM.

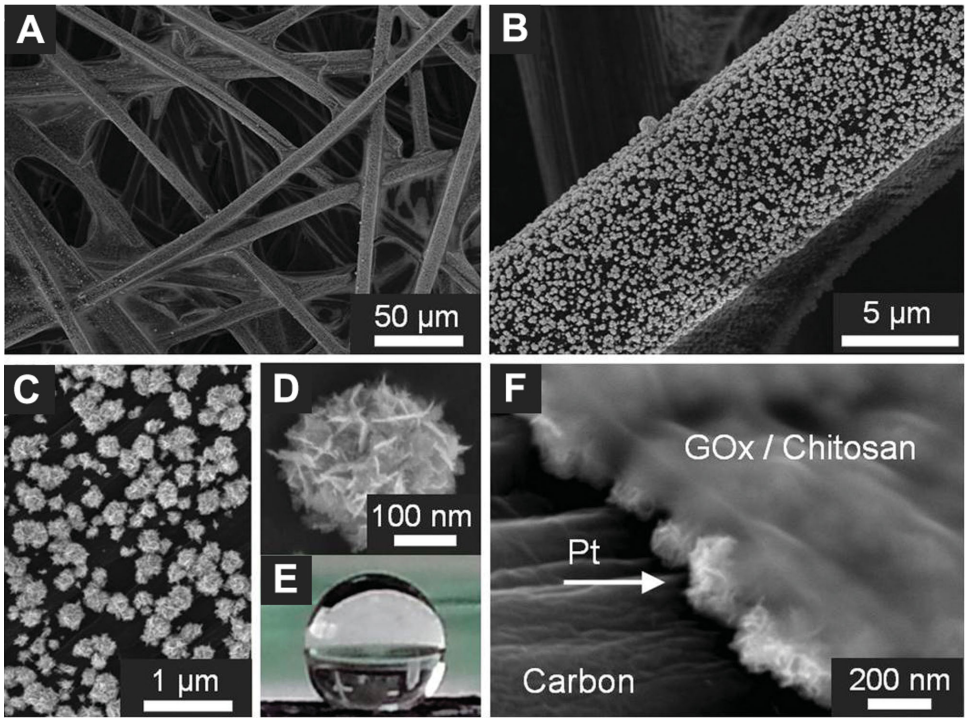

Figure 2. Surface morphologies of STP-biosensor. a–c) FE-SEM images of Pt particles decorated conducting superhydrophobic carbon fiber substrate at different magnifications. The diameter of carbon fibers is about 10 μm and form net-structures. Pt particles with sizes range from 50 to 300 nm distribute homogeneously on the surface of the topmost layer of fibers. d) A typical hierarchical Pt particle that composed of nanoflakes with thickness of about 9 nm. e) Profile of a spherical water droplet suspended on the substrate. f) E-SEM image of the thin GO*x*/chitosan composite film coated on electrode substrate. Such architecture facilitates free diffusion of oxygen and glucose to the three-phase bioassay interface.

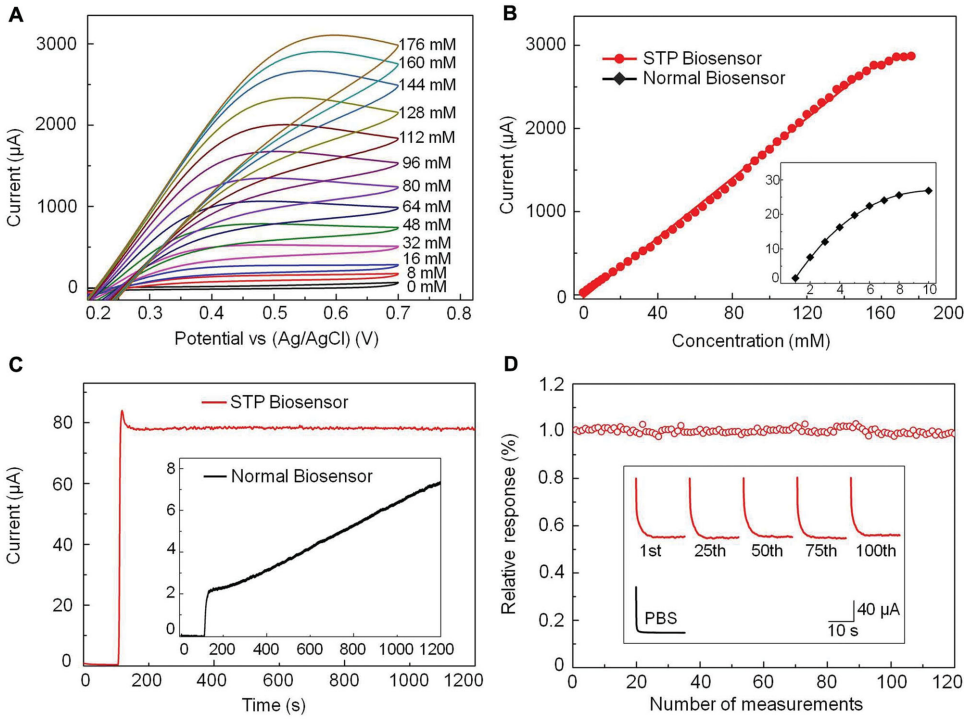

Figure 3. Performance of STP-biosensor for glucose detection. a) CVs corresponding to the electroxidation of glucose on STP-biosensor in the presence of glucose with various concentrations. b) Calibration plot derived from the CVs at +0.5 V versus Ag/AgCl. The linear detection upper limit is 156 mM, about 30 times higher than that obtained on normal biosensor (~5 mM) (inset in b). c) Amperometric response of STP-biosensor and normal biosensor (inset in c) to 4 mM glucose upon the analyte solution switching from oxygen-deficit to oxygen-fluctuant conditions. The current output remains constant with time for STP-biosensor but keeps increasing for normal one. This confirmed that oxygen level variation has no influence on the detection accuracy of STP-biosensor. d) Successive 120 measurements of 20 mM glucose. The relative standard deviation is 1.1%. Inset in (d) shows typical chronoamperometric responses as a function of time. The current responds rapidly and reaches a steady state in 5 s each time. The relative responses (%) are calculated by normalizing the current to the initial current obtained at 5 s following the potential step.

This confirmed that the oxidase kinetics is no longer oxygen level limited, so that wide linear detection range and good sensitivity were achieved simultaneously.

We further investigated the influence of oxygen level fluctuation in analyte solution on the detection accuracy of STP-biosensor. Prior to the assay of glucose solution with 4 mM concentration, oxygen in the analyte solution was removed by purging with argon for 40 min. As shown in the inset of Figure 3c, for normal biosensor, the current output is low and keeps increasing with time. This can be ascribed to the slow oxygen level increase caused by its diffusion from air under stirring condition, indicating that oxygen level fluctuation has a strong impact on the detection accuracy of normal biosensor. It is worth to note that oxygen level variation also influence the detection accuracy of artificial mediator based biosensors, in particular, while measuring analyte at low concentration. This can be attributed to oxygen interference because of the much faster reaction rate of oxygen-oxidase in comparison to rate of most artificial mediator–oxidase reactions.[27,28] which will show parasitic effect on sensor response. In marked contrast, the current output of STP-biosensor is about 160-fold higher and remains constant with time (Figure 3c). These results confirmed that the oxygen involved in oxidase-catalytic bioreaction at the assay interface of STP-biosensor is supplied constantly and sufficiently from air phase, so that the detection accuracy is insensitive to the oxygen level variation in analyte solution.

In addition to the wide linear detection range, good sensitivity and accuracy, other important aspects of STP-biosensor were further characterized. Figure 3d shows 120 times successive measurement of 20 mM glucose concentration using the same biosensor. A relative standard deviation of only 1.1% was observed for these measurements, indicating good repeatability. Moreover, as shown in the inset of Figure 3d, the biosensor responds rapidly and the current reaches a steady state within 5 s each time. The fast response of STP-biosensor can be attributed to the barrier-free influx of glucose to the assay interface, which is unlike normal biosensor, where analyte mass-transport-limiting membrane has to be used because of the low oxygen level in solution. The long-term stability of STP-biosensor was also studied by testing its response to 30 mM glucose for more than eight months. The results are shown in Figure S3 of the Supporting Information. The STP-biosensor retains its high activity over the course of 250 d with minor variation of less than 5%, caused primarily by slight environmental and operational variation from one test to another.

In principle, the STP-biosensor demonstrated here is applicable to other oxidase-based bioassays. We have measured sucrose, lactate and choline levels by using their corresponding oxidase-based STP-biosensors. Their linear detection ranges are all about an order of magnitude wider than those obtained on normal biosensors as shown in **Figure 4** and Figure S4 of the Supporting Information, suggesting that STP-biosensor

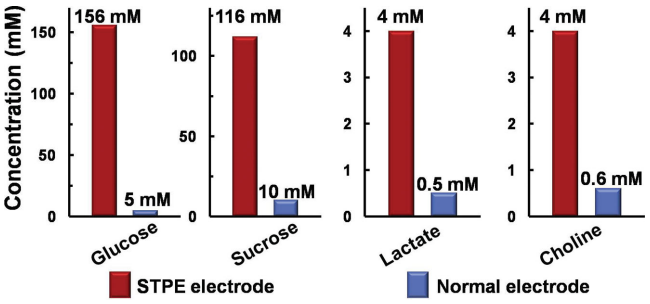

Figure 4. Performance of STP-biosensor in other oxidase-based bioassays. Comparison of linear detection upper limits of STP- and normal biosensors for glucose, sucrose, lactate, and choline assay, respectively. Linear detection ranges of STP-biosensor based assays are all about an order magnitude higher than those of normal ones.

can be potentially used for measurement of a wide range of clinically important substrates. We have also applied STP-biosensor to assay glucose in serum. Without dilution, linear detection up limit of ≈80 mM was achieved, which has never been achieved before as shown in Figure S5 of the Supporting Information.

In conclusion, we have demonstrated a facile approach for achieving high performance enzyme biosensor based on superhydrophobic electrode that has solid–liquid–air three phases interface, where oxygen is sufficient and constant. The oxygen-rich biosensor simultaneously realized the requirements for bioassay including wide linear detection range, good sensitivity and accuracy. We have also demonstrated that such electrode is generally applicable to the fabrication of other STP-biosensors, given the availability of a wide variety of oxidases, assaying approaches, superhydrophobic substrates and H_2O_2 catalysts. The results indicate that the superhydrophobic surface offers a unique route to address the gas-deficit problem of many reaction systems.

Experimental Section

Based on the design model, many types of STP-biosensors can be prepared depending on the assaying targets and approaches. Consequently, a wide variety of oxidases (GOx, LOx, etc.), superhydrophobic substrates (conducting or nonconducting), and H_2O_2 catalysts (metal, artificial peroxidase, heme proteins, carbon nanotube, graphene, or fluorescence probe) can be used. In this work we fabricated electrochemical STP-biosensor by immobilizing oxidases on Pt catalyst modified conducting superhydrophobic carbon fiber electrode subsdtate. Conducting carbon fiber substrate is ≈100 μm thick and has fiber diameter of ≈10 μm. Pt catalysts were potentiostatically deposited on one side of the substrate at –0.3 V versus Ag/AgCl for 100 s using a H_2PtCl_6 solution (10 g L^{-1} $HPtCl_6$:H_2O:1 M H_2SO_4 = 13:12:25, v:v:v). Solutions of oxidase (1 wt% in PBS solution), chitosan (1 wt% in acetic acid), and glutaraldehyde (25 wt% in DI water) was mixed thoroughly with a volume ratio of 10:10:3. The missed solution was then drop cast onto the Pt decorated substrate and dried naturally. Normal biosensor based on glassy carbon electrode (3 mm o.d.) was prepared in a similar way. Oxidases used here are glucose oxidase (EC 1.1.3.4, 126000 U g^{-1}, obtained from Toyobo Co., Ltd.), lactate oxidase (EC 1.1.3.2, 40000 U g^{-1}, obtained from Sigma), invertase (EC 3.2.1.26, 300000 U g^{-1}, obtained from Sigma) and choline oxidase (EC 1.1.3.17, 10000 U g^{-1}, obtained from Sigma). Analytes of glucose, lactate, sucrose, and choline were all obtained from Sigma and used without purification.

Surface morphologies of Pt catalyst modified electrode substrates were characterized using FE-SEM (HITACHI-S4800, Japan). Surface morphologies of oxidase/chitosan composite film coated electrode substrate were characterized using E-SEM (FEI Quanta 400 FEG, USA). Electrochemical experiments were performed with CHI-660e work station (CH Instruments, Inc). Ag/Ag/Cl and Pt wire were used, respectively, as reference electrode and counter electrode. A stirring rate of 300 rpm was maintained during all measurements. Chronoamperometric experiments were performed by measuring the current at 20 s following the potential step. Cyclic voltammetric and amperometric experiments were performed by applying a potential of +0.5 V versus Ag/AgCl, allowing a constant background current to be obtained, and adding the desired concentration of analytes. The current difference was recorded and used to plot the current–concentration curves.

Supporting Information

Supporting Information is available from the Wiley Online Library or from the author.

Acknowledgements

Y.L. and R.S. contributed equally to this work. This work was supported by the National Natural Science Foundation of China (21371178) and the Chinese Thousand Youth Talents Program (YZBQF11001).

Received: July 21, 2015
Revised: October 28, 2015
Published online: December 12, 2015

[1] W. Barthlott, C. Neinhuis, *Planta* **1997**, *202*, 1.
[2] L. Feng, S. H. Li, Y. S. Li, H. J. Li, L. J. Zhang, J. Zhai, Y. L. Song, B. Q. Liu, L. Jiang, D. B. Zhu, *Adv. Mater.* **2002**, *14*, 1857.
[3] A. Lafuma, D. Quéré, *Nat. Mater.* **2003**, *2*, 457.
[4] H. Y. Erbil, A. L. Demirel, Y. Avci, O. Mert, *Science* **2003**, *299*, 1377.
[5] X. Deng, L. Mammen, H. J. Butt, D. Vollmer, *Science* **2012**, *335*, 67.
[6] T. L. Liu, C.-J. C. Kim, *Science* **2014**, *346*, 1096.
[7] Y. Lu, S. Sathasivam, J. Song, C. R. Crick, C. J. Carmalt, I. P. Parkin, *Science* **2015**, *347*, 1132.
[8] X. J. Feng, L. Jiang, *Adv. Mater.* **2006**, *18*, 3063.
[9] K. S. Liu, X. Yao, L. Jiang, *Chem. Soc. Rev.* **2010**, *39*, 3240.
[10] Y. Tian, B. Su, L. Jiang, *Adv. Mater.* **2014**, *26*, 6872.
[11] T. S. Wong, S. H. Kang, S. K. Y. Tang, E. J. Smythe, B. D. Hatton, A. Grinthal, J. Aizenberg, *Nature* **2011**, *477*, 443.
[12] M. Paven, P. Papadopoulos, S. Schöttler, X. Deng, V. Mailënder, D. Vollmer, H. J. Butt, *Nat. Commun.* **2013**, *4*, 2512.
[13] Z. Y. Lu, W. Zhu, X. Y. Yu, H. C. Zhang, Y. J. Li, X. M. Sun, X. W. Wang, H. Wang, J. M. Wang, J. Luo, X. D. Lei, L. Jiang, *Adv. Mater.* **2014**, *26*, 2683.
[14] L. Wen, Y. Tian, L. Jiang, *Angew. Chem. Int. Ed.* **2015**, *54*, 3387.
[15] J. M. Wang, Y. M. Zheng, F. Q. Nie, J. Zhai, L. Jiang, *Langmuir* **2009**, *25*, 14129.
[16] L. C. Clark, C. Lyons, *Ann. N.Y. Acad. Sci.* **1962**, *102*, 29.
[17] S. J. Updike, G. P. Hicks, *Nature* **1967**, *214*, 986.
[18] G. G. Guilbaul, G. J. Lubrano, *Anal. Chim. Acta.* **1973**, *64*, 439.
[19] A. E. G. Cass, G. Davis, G. D. Francis, H. A. O. Hill, W. J. Aston, I. J. Higgins, E. V. Plotkin, L. D. L. Scott, A. P. F. Turner, *Anal. Chem.* **1984**, *56*, 667.
[20] A. Heller, *Acc. Chem. Res.* **1990**, *23*, 128.
[21] Y. Xiao, F. Patolsky, E. Katz, J. F. Hainfeld, I. Willner, *Science* **2003**, *299*, 1877.

[22] C. S. Shan, H. F. Yang, J. F. Song, D. X. Han, A. Ivaska, L. Niu, *Anal. Chem.* **2009**, *81*, 2378.
[23] H. L. He, X. L. Xu, H. X. Wu, Y. D. Jin, *Adv. Mater.* **2012**, *24*, 1736.
[24] L. C. Clark, *Patent US* **1988**, 4721677.
[25] J. Wang, F. Lu, *J. Am. Chem. Soc.* **1998**, *120*, 1048.
[26] E. L. Cussler, *Diffusion: Mass Transfer in Fluid Systems*, 2nd ed., Cambridge University Press, New York **1997**.
[27] J. Wang, J. W. Mo, S. F. Li, J. Porter, *Anal. Chim. Acta.* **2001**, *441*, 183.
[28] G. Kenausis, C. Taylor, I. Katakis, A. Heller, *J. Chem. Soc., Faraday Trans.* **1996**, *92*, 4131.